IUST
Iran University of Science and Technology

Iranian Journal of Electrical and Electronic Engineering

Journal Homepage: ijeee.iust.ac.ir

Integrating Deep Transfer Learning and Image Enhancement for Enhancing Defective Photovoltaic Cells Classification in Electroluminescence Images

Hanim Suraya Mohd Mokhtar*, Aimi Salihah Abdul Nasir**(C.A.) , Mohammad Faridun Naim Tajuddin**, Muhammad Hafeez Abdul Nasir*** and Kumuthawathe Ananda Rao**

Abstract: The rapid growth of photovoltaic (PV) systems has highlighted the need for efficient and reliable defect detection to maintain system performance. Electroluminescence (EL) imaging has emerged as a promising technique for identifying defects in PV cells; however, challenges remain in accurately classifying defects due to the variability in image quality and the complex nature of the defects. Existing studies often focus on single image enhancement techniques or fail to comprehensively compare the performance of various image enhancement methods across different deep learning (DL) models. This research addresses these gaps by proposing an in-depth analysis of the impact of multiple image enhancement techniques on defect detection performance, using various deep learning models of low, medium, and high complexity. The results demonstrate that mid-complexity models, especially DarkNet-53, achieve the highest performance with an accuracy of 94.55% after MSR2 enhancement. DarkNet-53 consistently outperformed both lower-complexity models and higher-complexity models in terms of accuracy, precision, and F1-score. The findings highlight that medium-depth models, enhanced with MSR2, offer the most reliable results for photovoltaic defect detection, demonstrating a significant improvement over other models in terms of accuracy and efficiency. This research provides valuable insights for optimizing defect detection systems in photovoltaic applications, emphasizing the importance of both model complexity and image enhancement techniques for robust performance.

Keywords: Photovoltaic (PV), Defect Classification, Electroluminescence, Multi-Scale Retinex (MSR), Multi-Scale Retinex 2 (MSR2), Pre-Trained Models

1 Introduction

IN recent years, solar photovoltaic (PV) energy garnered substantial attention due to the growing importance of clean and sustainable energy resources. Solar PV systems are widely recognized for their potential to address global energy challenges by reducing dependence on fossil fuels and minimizing greenhouse gas emissions. As the core component of solar panels, PV cells play a pivotal role in converting sunlight into electrical power, making them essential in achieving high-efficiency energy solutions. The rapid adoption of solar PV technology underscores its significance in fostering energy independence and mitigating climate change.

Defects in PV cells, such as cracks, hotspots, and material degradation, can significantly compromise the efficiency and reliability of solar panels [1]. These defects, whether originating from manufacturing flaws

Iranian Journal of Electrical & Electronic Engineering, 2025.
Paper first received 01 Dec 2024 and accepted 18 Feb 2025.
* The author is with the Faculty of Electrical Engineering & Technology, Universiti Malaysia Perlis (UniMAP), 02600 Arau, Perlis, Malaysia.
** The authors are with the Centre of Excellence for Renewable Energy (CERE), Universiti Malaysia Perlis (UniMAP), 02600 Arau, Perlis, Malaysia.
*** The author is with the School of Housing, Building and Planning, Universiti Sains Malaysia (USM), 11700 Gelugor, Pulau Pinang, Malaysia.
E-mail: aimisalihah@unimap.edu.my
Corresponding Author: Aimi Salihah Abdul Nasir

or environmental stresses, necessitate accurate identification and classification to ensure optimal solar energy system performance. Effective defect detection often relies on image-based diagnostic techniques like electroluminescence (EL) imaging. However, the quality of these images plays a critical role in successful defect classification. Challenges such as low contrast, uneven illumination, and noise frequently obscure defects, complicating the analysis process. To address these issues, advanced image enhancement techniques are employed to improve the visibility of defect regions, enabling more accurate and reliable classification using state-of-the-art methods like deep learning models.

Advanced imaging techniques, combined with sophisticated image processing and machine learning algorithms, offer solutions for the effective classification of PV cell defects. By accurately identifying and categorizing these defects, such approaches enable timely interventions, ensuring the long-term efficiency and reliability of solar energy systems. Fig. (1) illustration of common PV cell defects, including finger interruptions, dislocations, printing errors, star cracks, short circuits, line cracks, and black cores, which disrupt electrical pathways and indicate potential structural weaknesses. In contrast, non-defective PV cells exhibit uniform surface texture, consistent crystalline patterns, even illumination, and an absence of visible imperfections.

Fig. 1(a) shows a finger interruption, which disrupts electrical pathways and lowers energy efficiency. Fig. 1(b) and 1(c) illustrate horizontal and vertical dislocations, indicating structural weaknesses that can lead to mechanical instability. Fig. 1(d) depicts a printing error from manufacturing flaws, affecting material consistency and cell performance. Fig. 1(e) shows a star crack that weakens the cell and makes it more susceptible to environmental damage. Fig. 1(f) illustrates a short circuit, causing current to bypass parts of the cell and reducing efficiency. Fig. 1(g) depicts a line crack, which compromises both mechanical and electrical performance. Fig. 1(h) shows a black core, indicating severe damage or contamination that reduces output. Fig. 1(i) and (j) display non-defective PV cells with uniform texture and no visible issues. These defects, from manufacturing or operational stress, critically affect the functionality and durability of PV cells.

EL imaging is an effective diagnostic tool for detecting and analyzing defects in PV cells. By applying a forward bias, the PV cell emits light, captured by a specialized camera, revealing micro-cracks, finger interruptions, and other subtle defects invisible to the naked eye or conventional methods. EL images offer a detailed view of the cell's internal structure and condition, aiding in precise defect identification and classification. The high contrast and resolution of EL images are crucial for quality control in manufacturing and assessing the health of operational solar panels. Advanced image processing and machine learning algorithms can further utilize EL imaging data to improve the reliability and performance of PV systems.

Given its ability to provide detailed views of PV cells' internal structures, EL imaging has become a widely adopted technique among researchers and practitioners for defect detection in solar PV systems. Numerous studies have demonstrated the effectiveness of EL imaging in identifying defects using conventional methods. The high resolution and contrast offered by EL images make them invaluable for both manufacturing quality control and the assessment of operational solar panels. As a result, EL imaging has been extensively used as a primary diagnostic tool in combination with advanced image processing and machine learning algorithms to enhance the accuracy and reliability of defect classification, contributing to the overall optimization of PV system performance.

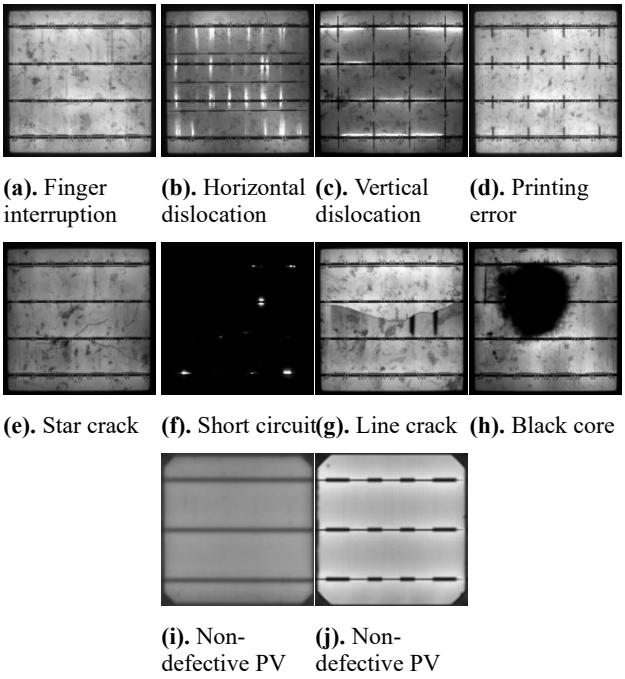

(a). Finger interruption **(b).** Horizontal dislocation **(c).** Vertical dislocation **(d).** Printing error

(e). Star crack **(f).** Short circuit **(g).** Line crack **(h).** Black core

(i). Non-defective PV **(j).** Non-defective PV

Fig 1. Examples of various PV cell conditions.

To ensure accurate detection and classification of defects in PV cells, the quality of diagnostic images, such as EL images, must be sufficient to reveal subtle imperfections. However, raw images often suffer from limitations like low contrast, uneven illumination, and noise, which can obscure critical details. Addressing these challenges requires the application of image enhancement techniques, which play a pivotal role in improving the visual clarity and informativeness of PV images.

Image enhancement is the process of improving the visual quality of an image, aiming to make it clearer and more informative for easier identification and analysis of important features. This involves techniques like contrast enhancement, noise reduction, image sharpening, and illumination normalization. In PV cells, image enhancement is crucial because images from PV modules, such as EL images, often have low quality due to issues like low contrast, uneven illumination, and noise. These problems can hide defects like cracks, finger interruptions, and dislocations. By improving image quality, enhancement techniques make these defects more visible and easier to detect and classify. Enhanced images help defect detection algorithms work more effectively, increasing the accuracy of defect detection in PV modules. Early identification and repair of defects ensure the efficiency and reliability of PV systems, which is vital for their long-term performance.

Several studies have been conducted to apply image enhancement techniques to PV images, particularly for defect detection in solar cells. For instance, Zotin et al. [2] developed a Fast Multiscale Retinex algorithm to enhance colour images, which can be applied to PV images to improve contrast and illumination. Another research, Lee et al. [3] proposed using an Adaptive Multiscale Retinex to enhance image contrast, aiding in the detection of defects in PV images. Additionally, the study in Fan et al. [4] introduced an image enhancement algorithm to determine the dust level on PV panels, a factor that can affect panel performance. Furthermore, Meng et al. [5] reviewed traditional methods for defect detection and image enhancement in solar cells, illustrating how these techniques can be used to improve PV images. These studies demonstrate the critical role of image enhancement in ensuring that PV images are of sufficient quality for accurate defect detection and classification.

While image classification focuses on identifying and categorizing objects within an image, another crucial step in the analysis of PV images is image segmentation. This process delves deeper by dividing an image into distinct regions or segments, enabling more precise localization and identification of defects within PV cells. Image classification involves identifying and categorizing objects within an image into predefined classes, utilizing methods like pre-trained models and Convolutional Neural Networks (CNN). Pre-trained models, trained on large datasets, can recognize various patterns and features in images. CNN, designed to process grid-like data, use convolutional layers to extract important features, pooling layers for down sampling, and fully connected layers for making predictions. This architecture effectively captures spatial hierarchies and local patterns, making it ideal for image classification tasks.

Deep learning has emerged as a powerful tool in defect detection across various fields, including solar PV systems. Leveraging neural network architectures such as CNN and their advanced variants, deep learning enables the automated extraction of complex features from images, surpassing traditional image processing techniques in accuracy and efficiency. In recent years, the application of deep learning to EL images have gained significant attention due to its ability to analyze high-resolution diagnostic data and identify subtle defects like micro-cracks, hotspots, and finger interruptions.

This trend is reflective of the broader adoption of deep learning in diverse image classification tasks, including medical diagnostics, autonomous vehicles, and industrial quality control. For solar PV defect detection, the integration of deep learning algorithms with EL imaging provides an advanced framework for accurate and reliable classification, ensuring improved efficiency and reliability of PV systems. As a result, many researchers have focused on applying deep learning techniques to EL images, recognizing its potential in enhancing defect detection capabilities and addressing the growing demand for sustainable energy solutions.

In the field of PV solar panel defect detection, the use of transfer learning with deep CNN has demonstrated considerable potential. Various studies have explored this approach, demonstrating its effectiveness in identifying surface defects in solar panels. For instance, Zyout et al. [6] applied transfer learning with the AlexNet model to characterize and detect surface defects on PV solar panels. Their analysis focused on standard images of solar panel surfaces, rather than EL images. The accuracy achieved in the defect detection process using the AlexNet model was reported to be 92.0%, showcasing the potential of transfer learning and deep learning models in advancing surface defect detection for solar PV systems. Additionally, Li et al. [7] proposed an improved VGG-19 pre-trained model for defect detection, outperforming classical VGG19 in accuracy, precision, recall rate, and F1 score. The study's emphasis on transfer learning and hierarchical feature fusion contributed to the enhanced defect detection performance, showcasing the effectiveness of the improved network architecture. Next, the proposed model was tested on two publicly available global datasets of PV defective EL images. For comparative benchmarking, various CNN including VGG-16, MobileNet-V2, Inception-V3, DenseNet-121, ResNet-152, Xception, and InceptionResNet-V2 were utilized. The evaluation demonstrated significant improvements in several metrics. The model achieved an accuracy of 96.17% in the binary classification task of identifying the presence or absence of defects, and 92.13% in the

multiclass classification task of identifying different defect types.

Next, the categorization of photovoltaic defect detection using EL images depends heavily on deep learning. Deitsch et al. [8] conducted pioneering research by applying CNN models to EL image analysis. This researcher trained a CNN model that achieved an impressive accuracy of 88.42%, outperforming the SVM model used in their study. Subsequently, Akram et al. [9] enhanced this work by employing data augmentation techniques and developing a lightweight CNN model that achieved even higher accuracy, reaching 93.02%. However, these models are primarily focused on binary classification which is functional or defective and do not address specific defect categorization.

Karimi et al. [10] developed a comprehensive pipeline for processing EL images. Initially, raw EL images underwent automatic transformation and cropping to extract individual cell images. This research subsequently trained three models which are Random Forest (RF), Support Vector Machine (SVM), and CNN to classify cells into categories such as good, cracked, and corroded. The CNN model demonstrated superior performance, achieving an impressive accuracy of 99.71% on their test dataset. The automated preprocessing tool represents a significant advancement. However, it necessitates additional validation using field images that may contain more complex backgrounds.

Mayr et al. [11] utilized ResNet-50 as the backbone and a normalized layer for semantic segmentation to detect cracks at the pixel level in cell images. In a similar vein, Fioresi et al. [12] employed a Deeplabv3 model with ResNet-50 backbone for crack segmentation, achieving an impressive weighted F1-score of 95.00%.

In summary, this research aims to enhance the identification and classification of defective and non-defective PV cells by leveraging advanced image enhancement techniques and deep learning algorithms. Previous studies have shown promising results in defect detection using deep learning models on EL images; however, few have explored the application and comparative analysis of different image enhancement methods. This study addresses this gap by analyzing the impact of various image enhancement techniques on deep learning model performance. Specifically, it compares models of varying complexities—low, medium, and high-depth architectures. Additionally, this research utilizes a large number of EL images from diverse datasets to evaluate the performance of the models in different contexts. The key contributions of this study include a comprehensive analysis of image enhancement methods, a comparison of deep learning models with different depths, and the use of multiple datasets to assess model robustness. These efforts promise to improve defect detection accuracy and efficiency, thus enhancing the reliability and performance of PV systems, ultimately contributing to more effective solar energy generation.

2 Methodology

In this study, we utilized 10,000 photovoltaic EL images from four datasets, equally divided between 5, 000 defective and 5,000 non-defective cells. The diverse range of EL images representing various defect types highlights the effectiveness of transfer learning techniques in addressing this critical challenge. To enhance the images, we compared two image enhancement techniques: Multi-Scale Retinex (MSR) and MSR2. These enhanced images were then fed into ten distinct types of deep learning models: CNN, AlexNet, DarkNet-53, DenseNet-201, EfficientNet-b0, GoogLeNet, ResNet-101, SqueezeNet, VGG-19 and Xception. The models' architectures were developed using MATLAB R2023b and executed on a graphical processing unit (GPU), specifically the NVIDIA GeForce RTX.

2.1 Dataset Overview of Electroluminescence Images

This research leverages multiple publicly available online datasets to evaluate the performance of deep learning models for defect detection and classification in PV cells. By utilizing datasets from diverse sources, including GitHub and the EMN Data Hub, the study aims to measure the generalizability and robustness of the models across different defect patterns and imaging conditions. Such diversity ensures that the findings are applicable to real-world scenarios where variations in image quality, lighting conditions, and defect types are common.

Table 1 summarizes the datasets used in this study, including their sources, the total number of images available, the subset of images utilized, and the classification of defective versus non-defective images. The ELPV Dataset [8], [13], [14], sourced from GitHub, comprises 2,624 photovoltaic EL images, with all images being used in this study. This dataset includes 1,116 defective cells and 1,508 non-defective cells. The UCF-EL Defect Dataset [12], also obtained from GitHub, originally contains 17,064 EL images. For our research, we selected a subset of 4,420 images, consisting of 1,310 defective and 3,110 non-defective cells. The Crack Segmentation Dataset from the EMN Data Hub includes a total of 2,159 images. From this dataset, 1,956 images were used, which include 1,574 defective cells and 382 non-defective cells. Lastly, the Photovoltaic Electroluminescence Anomaly Detection Dataset [15], [16], [17], [18] from GitHub provides 36,543 near-infrared images with various internal defects and diverse backgrounds. For our study, we selected 1,000 defective cells from this dataset. This

comprehensive overview of the datasets highlights the variety and scope of the images used for defect detection and classification in photovoltaic cells.

Table 1. Summary of datasets used in this study.

Dataset	Source	Total Images Available	Total Images Used	Defective Images	Non-Defective Images
ELPV Dataset [8], [13], [14]	GitHub	2,624	2,624	1,116	1,508
UCF-EL Defect Dataset [12]	GitHub	17,064	4,420	1,310	3,110
Crack Segmentation Dataset	EMN Data Hub	2,159	1,956	1,574	382
Photovoltaic Electrolumines-cence Anomaly Detection Dataset [15], [16], [17], [18]	GitHub	36,543	1,000	1,000	-

2.1.1 Dataset Distribution for Training and Validation

To effectively train and evaluate the performance of our models, we organized the total dataset of 10,000 photovoltaic EL images into training and validation subsets. Specifically, 60% of the images were allocated for training, while the remaining 40% were reserved for validation. Before splitting the dataset, we ensured that the images were randomized to avoid any potential bias in the selection process. This randomization was crucial to ensure that both subsets were representative of the overall dataset, promoting unbiased learning.

Table 2 outlines the distribution of our datasets into training and validation sets for the research of defect detection in photovoltaic cells using EL images. For the training phase, we allocated 6,000 images, with 3,000 images belonging to the defective class and 3,000 to the non-defective class. This balanced distribution ensures that the model receives equal exposure to both types of images, promoting better learning and reducing the risk of bias toward either class. For the validation phase, which is crucial for evaluating the model's performance and tuning its parameters, we used 4,000 images. This set also maintains an even split, with 2,000 defective images and 2,000 non-defective images. By keeping the validation dataset balanced, we can accurately assess the model's ability to generalize and correctly classify new, unseen images.

Table 2. The arrangements of training and validation datasets.

Dataset / Class	Defective	Non-Defective	Total
Training	3,000	3,000	6,000
Validation	2,000	2,000	4,000
Total	5,000	5,000	10,000

In summary, the dataset is carefully divided into training and validation sets to provide a robust framework for developing and evaluating our defect detection models. This balanced approach ensures that the models are well-trained, and their performance is reliably assessed. Moreover, utilizing a large dataset is crucial for this study as it enhances the generalizability of the models, reducing the risk of overfitting and ensuring reliable performance on unseen data. A larger dataset captures a broader range of variations and defect patterns, which is essential for robust defect detection in real-world scenarios. By avoiding the limitations of small datasets, the study aims to achieve higher accuracy and better reliability in classifying photovoltaic cell defects.

2.2 Image Enhancement for Electroluminescence Images

This research employs and analyzes two advanced image enhancement techniques, Multi-Scale Retinex (MSR) and Modified Multi-Scale Retinex (MSR2) to improve the quality and interpretability of EL images. EL images are inherently challenging due to issues such as low contrast, uneven illumination, and noise, which can obscure critical defect patterns. Image enhancement is applied in this study to address these challenges by improving contrast, highlighting subtle features, and ensuring uniform brightness, thereby enabling accurate defect detection and classification.

Multi-Scale Retinex (MSR) [19] is an advanced image enhancement technique designed to improve the visual quality of images by addressing issues of dynamic range compression, colour constancy, and colour rendition. It is particularly effective in enhancing images captured under varying lighting conditions. MSR was developed to overcome the limitations of the Single Scale Retinex (SSR) method, especially in balancing dynamic range compression and colour rendition. Retinex theory, which is rooted in human visual perception, aims to achieve colour constancy and dynamic range compression. MSR enhances this concept by combining multiple SSR outputs at different scales to provide a more balanced enhancement. The MSR algorithm calculates a weighted sum of the SSR outputs, which allows for improved local dynamic range and colour rendition. This multi-scale approach ensures that the enhanced image

maintains both fine and coarse details, achieving a visually pleasing balance between dynamic range and colour accuracy.

Based on the study conducted by Shaari et.al, [19], Eq. (1) presents the MSR formula, where represented the number of scales, denotes the weight of each scale, serves as the normalization factor, denotes input image on the colour channel and $F_n(x,y) = C_n exp\left[-\frac{(x^2+y^2)}{2\sigma_{n^2}}\right]$.

$$R_{MSR_i} = \sum_{n=1}^{N} w_n R_n = \sum_{n=1}^{N} w_n \left[log\, I_i(x,y) - log\big(F_n(x,y) \cdot I_i(x,y)\big)\right] \quad (1)$$

Then, Zhou et.al [20] further refine and improve the MSR technique, where MSR2 was developed, which accepts different desired scales as input and permits non-constrained scaling. MSR2 is an extension of the original MSR algorithm that incorporates additional processing steps to enhance its performance. The key improvements in MSR2 include more sophisticated noise reduction techniques and adaptive parameter tuning, which allows the algorithm to better handle different types of images and lighting conditions.

The enhanced MSR2 algorithm follows a structured process to achieve superior image enhancement. First, it performs multi-scale decomposition using Gaussian filters at different scales to capture fine and coarse details effectively. Next, noise reduction is applied, utilizing advanced techniques to suppress noise and minimize artifacts during the enhancement process. Following this, adaptive parameter tuning adjusts the algorithm's parameters dynamically based on the input image's characteristics, ensuring robust and flexible performance across varying conditions. Finally, the outputs from different scales are combined and reconstructed using a weighted sum approach, followed by post-processing steps to further enhance the overall visual quality of the image.

The development of MSR2 addresses some of the limitations of the original MSR algorithm, offering improved noise management and adaptive capabilities tailored for diverse imaging conditions. This makes MSR2 particularly effective for enhancing solar cell EL images, where high-quality enhancement is critical for accurately identifying subtle defects, improving defect classification, and ensuring reliable analysis in photovoltaic applications.

2.3 Leveraging CNN and Deep Pre-Trained Networks for Electroluminescence Image Classification

In this section, we detail the model architectures and training configurations used for classifying EL images of photovoltaic cells. Our approach involved both CNN and pre-trained models, each tailored to enhance defect detection capabilities.

2.3.1 Description of CNN and Pre-Trained Models

In this study, we utilized a baseline CNN and several pre-trained models categorized into three groups based on network depth: lower-depth models (AlexNet, SqueezeNet, EfficientNet-b0), medium-depth models (GoogLeNet, DarkNet-53, VGG-19), and higher-depth models (DenseNet-201, ResNet-101, Xception). Lower-depth models, typically consisting of 5 to 20 layers, are lightweight and computationally efficient, making them well-suited for applications with limited resources or small datasets, though their shallower architecture can limit their ability to learn complex features. Medium-depth models, with 20 to 100 layers, offer a balance between computational efficiency and representational power, making them ideal for tasks requiring moderate complexity. Higher-depth models, with over 100 layers, excel in tasks requiring the extraction of complex, hierarchical features, though they demand significant computational resources; they often incorporate residual or dense connections to improve training efficiency and mitigate issues like vanishing gradients. This categorization allows for a systematic comparison of classification performance across models with varying complexities when applied to EL images of PV cells.

These pre-trained models were chosen for their established effectiveness in image classification tasks, making them well-suited for defect detection in photovoltaic cells. The study focuses on analyzing their performance without modification to provide insights into the inherent capabilities of these architectures when applied to the unique characteristics of EL images.

The decision to use a baseline CNN and pre-trained models without modifications was driven by the objective of establishing a foundational comparison. This approach ensures a fair evaluation of existing architectures, highlights their strengths and limitations, and provides a benchmark for future studies that may involve architectural modifications or task-specific enhancements. By maintaining this focus, the study aims to present a clear and objective analysis of classification performance.

Convolutional Neural Networks (CNNs) [21] are widely used for image processing tasks due to their ability to efficiently handle spatial data. They employ convolutional layers for feature extraction, pooling layers for down-sampling, and fully connected layers for predictions, making them ideal for tasks like image classification, object detection, and segmentation. While CNNs excel at capturing local patterns, they often struggle with long-range dependencies and semantic connections, requiring deeper architectures or additional mechanisms to handle such complexities.

AlexNet [6], one of the earliest deep CNN, made a significant impact on image classification tasks by

introducing key innovations that are now standard in modern deep learning models. It was among the first to use Rectified Linear Unit (ReLU) activation functions, which accelerated training by alleviating the vanishing gradient problem. The model also incorporated dropout to prevent overfitting by randomly disabling a subset of neurons during training, and it employed data augmentation techniques, such as image rotations and translations, to increase the diversity of the training data and improve generalization. The architecture consists of five convolutional layers followed by three fully connected layers, where the convolutional layers progressively extract features, and the fully connected layers combine them for classification. AlexNet's groundbreaking performance in the 2012 ImageNet competition established it as a foundational model in deep learning, influencing the design of subsequent CNNs and advancing the field of computer vision.

SqueezeNet [22] is designed with a lightweight architecture that prioritizes efficiency while maintaining strong performance. The model uses "fire modules," which combine 1x1 and 3x3 convolutional filters to drastically reduce the number of parameters compared to traditional architectures, making it more computationally efficient. Despite its smaller size, SqueezeNet retains competitive accuracy, which makes it particularly well-suited for resource-constrained environments, such as mobile devices or embedded systems, where processing power and memory are limited. This combination of efficiency and performance allows SqueezeNet to excel in applications that require a balance between speed and model effectiveness.

EfficientNet-b0 [23] uses a compound scaling method that uniformly adjusts depth, width, and resolution with fixed coefficients, balancing network dimensions for better performance and efficiency. It uses depth-wise separable convolutions to cut down on parameters and computational cost, allowing for high accuracy while being more resource-efficient. Neural Architecture Search (NAS) and AutoML techniques are used to automatically find the best network design, resulting in a highly efficient model that delivers top performance while using fewer computational resources.

GoogleNet [24], also known as Inception-v1, introduced the innovative Inception module, which utilizes multiple convolutional filter sizes in parallel. This approach allows the model to capture a wide range of features, from fine-grained details to more abstract patterns, in a single layer. By doing so, GoogLeNet reduces the computational cost typically associated with using large, deep networks, all while maintaining high classification accuracy. The modular design of the network also enables it to scale effectively, making it suitable for a variety of image recognition tasks. This balance of efficiency and accuracy has made GoogLeNet a widely adopted architecture in deep learning.

DarkNet-53 [25], with 53 convolutional layers, this deep network captures complex features from images, enabling it to learn detailed patterns and representations crucial for precise image classification and object detection. The architecture includes residual connections that ease the vanishing gradient problem and support the training of very deep networks by allowing gradients to flow more easily, enhancing learning efficiency and performance. Despite its complexity, Darknet-53 is designed to be computationally efficient, balancing accuracy and speed to suit real-time applications like object detection in the You Only Look Once (YOLO) framework.

VGG-19 [19], with 19 layers, including 16 convolutional layers and 3 fully connected layers, this network structure captures detailed and complex image features. The network uses 3x3 convolutional filters in all its layers to capture detailed spatial features and create a hierarchy of increasingly complex features. Uses a straightforward design with repeated convolutional and max-pooling layers, making it easy to implement and effective at learning spatial patterns in the data.

Similarly, DenseNet-201 [26], in a feed-forward manner, each layer is fully connected to every other layer, enhancing information flow, feature reuse, and gradient propagation, which supports the training of deeper networks. Reduces the number of parameters compared to traditional convolutional networks by using dense connections, which not only avoids the vanishing gradient problem but also enhances feature reuse without compromising performance. By combining Batch Normalization, ReLU activation, and Convolution operations in each layer, this approach improves learning efficiency and robustness, allowing the network to achieve high accuracy with fewer parameters and lower computational costs.

ResNet-101 [27], by using residual learning and skip connections, this network can be very deep (101 layers) while avoiding the vanishing gradient problem, as the skip connections help the network learn identity mappings, simplifying the training of deeper models. The network employs a bottleneck design with each residual block consisting of three layers (1x1, 3x3, and 1x1 convolutions), which cuts down on parameters and computational complexity while maintaining performance. With its deep architecture and residual learning framework, this model excels in generalization, consistently delivering high accuracy across diverse image classification tasks and datasets.

Finally, Xception [28] builds on the Inception architecture by incorporating depth-wise separable convolutions, a technique that significantly improves feature extraction efficiency. This approach separates the

process of filtering and combining features, allowing the model to focus on learning more meaningful and compact features while reducing the computational load. By enhancing parameter utilization, Xception not only improves performance but also achieves faster training times and better generalization. As a result, it demonstrates remarkable performance in both image classification and object detection tasks, making it highly effective for a variety of computer vision applications.

Collectively, these models represent a broad spectrum of innovations and design strategies in neural networks, each tailored to address specific challenges in image analysis. They demonstrate a variety of approaches, from lightweight architectures optimized for computational efficiency to deep models that excel in extracting complex features. These advancements reflect the ongoing evolution in the field of computer vision, where balancing accuracy, computational cost, and efficiency is crucial for practical real-world applications. By leveraging different techniques such as residual connections, depth-wise separable convolutions, and multi-scale processing, these models continue to push the boundaries of what is achievable in terms of both performance and resource utilization, making them invaluable for tasks like image classification, object detection, and beyond.

2.3.2 Training Parameters and Configuration

In this section, we detail the training parameters and configurations used for fine-tuning the various models employed in this study. These settings are crucial for optimizing the performance of both CNN and the pre-trained models on the photovoltaic defect detection. The choice of parameters, such as input image size, activation functions, and optimization methods, plays a significant role in how effectively each model learns and generalizes from the data.

Table 3 summarizes the fine-tuning parameters and configurations for the CNN and pre-trained models used in this study for photovoltaic defect detection from EL images. It includes information on input image size, activation functions, optimizers, and the number of training epochs. This table helps to illustrate how each model was tailored to achieve optimal performance for detecting defects in photovoltaic EL images.

For most models, the input image size was set to 224x224x3 pixels, while DarkNet-53 used a larger size of 256x256x3 pixels. This choice ensures compatibility with the respective architectures while balancing computational efficiency and detail preservation essential for accurate defect detection. Activation functions are crucial for introducing non-linearity into the models. The Rectified Linear Unit (ReLU) was predominantly used for its effectiveness in mitigating the vanishing gradient problem. DarkNet-53 used Leaky ReLU to better handle negative values, and EfficientNet-b0 employed the Swish activation function, which improves performance by allowing smoother gradients. Cross-entropy was used as the loss function across all models, facilitating effective learning by comparing predictions to actual labels. Stochastic Gradient Descent with Momentum (SGDM) was chosen as the optimizer for its efficiency in speeding up training and finding optimal solutions. Each model was trained for 25 epochs, a duration that strikes a balance between achieving high performance and avoiding overfitting.

Table 3. Fine tuning of the pre-trained models and CNN for photovoltaic detection from EL images.

Models	Size	Activation Function	Optimizer	Epoch
CNN	224x224x3	ReLU	SGDM	25
AlexNet	227x227x3	ReLU	SGDM	25
DarkNet-53	256x256x3	Leaky ReLU	SGDM	25
DenseNet-201	224x224x3	ReLU	SGDM	25
EfficientNet-b0	224x224x3	Swish	SGDM	25
GoogLeNet	224x224x3	ReLU	SGDM	25
ResNet-101	224x224x3	ReLU	SGDM	25
SqueezeNet	227x227x3	ReLU	SGDM	25
VGG-19	224x224x3	ReLU	SGDM	25
Xception	299x299x3	ReLU	SGDM	25

In summary, by fine-tuning these CNN and pre-trained models, aimed to improve defect detection in photovoltaic EL images. This detailed setup and optimization are pivotal in advancing the reliability and efficiency of photovoltaic systems.

2.3.3 Performances Evaluations Metrics

The performance of the classification models was assessed using five key metrics: validation accuracy, precision, sensitivity, specificity, and F1-score.

Table 4 provides the formulas used to calculate the performance evaluation metrics. These evaluation metrics are essential for a comprehensive evaluation of the model's performance in detecting defective and non-defective of photovoltaic EL images, ensuring that both the accuracy and reliability of the defect detection process are thoroughly assessed.

In this context, the number of defective photovoltaic EL images that were correctly recognized as defective is referred to as “true positive” (TP). The total number of non-defective photovoltaic EL images that were accurately identified as non-defective is represented by the term “true negative” (TN). On the other hand, “false

positive" (FP) explains conditions in non-defective photovoltaic EL images that are non-defective were mistakenly classified as defective. Finally, the term "false negative" (FN) describes the number of photovoltaic EL images that were found to be defective but were wrongly categorized as non-defective.

Table 4. Evaluation metrics.

Assessments	Formula
Accuracy	$\frac{TP+TN}{TP+TN+FP+FN}$
Precision	$\frac{TP}{TP+FP}$
Sensitivity	$\frac{TP}{TP+FN}$
Specificity	$\frac{TN}{TN+FP}$
F1-Score	$\frac{(2\cdot TP)}{(2\cdot TP)+FP+FN}$

In summary, the use of these performance metrics allows for a thorough understanding of how well the models distinguish between defective and non-defective photovoltaic EL images. By evaluating the models across multiple metrics, we ensure a robust analysis of their overall effectiveness in defect detection.

3 Results and Discussions

This section outlines the used to evaluate and enhance the performance of CNN and pre-trained models for classifying defective and non-defective photovoltaic EL images. The approach integrates image enhancement techniques with state-of-the-art deep learning models to achieve optimal accuracy in defect detection.

3.1 Qualitative Analysis of Image Enchancement

In this study, we assessed the effectiveness of MSR and MSR2, in enhancing the detection of defects in photovoltaic EL images. The analysis in Fig. 2 highlights why MSR2 is superior to MSR in this context.

The original non-defective photovoltaic EL image is depicted in Fig. 2(a), while Figs. 2(b) to (d) display original defective images showing line cracks, star cracks, and soiling, respectively. These images serve as the baseline, illustrating the inherent defects and quality of the photovoltaic cells before any enhancement is applied.

MSR was used to improve image clarity by enhancing details and reducing variations in illumination. Figs. 2(e) to (h) demonstrate the results of applying MSR, with the enhanced images showing clearer distinctions between defective and non-defective areas. The technique effectively highlights the features of the defects, improving their visibility. However, it also introduces some distortions—slight artifacts or exaggerations in certain parts of the image. While these distortions are noticeable, they do not significantly interfere with defect detection, allowing MSR to still be a useful tool in analyzing these images.

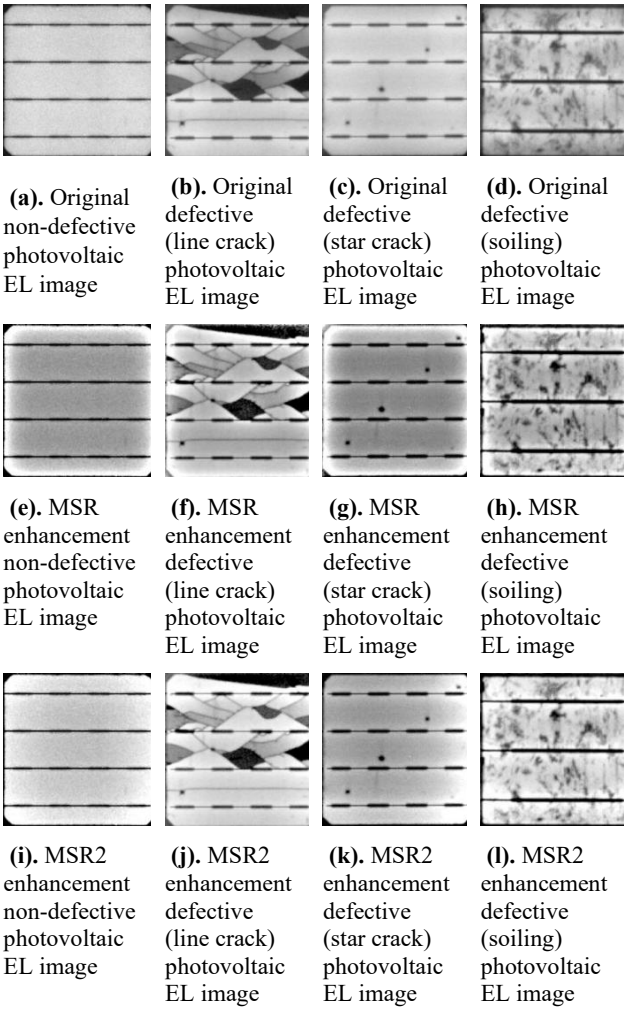

(a). Original non-defective photovoltaic EL image
(b). Original defective (line crack) photovoltaic EL image
(c). Original defective (star crack) photovoltaic EL image
(d). Original defective (soiling) photovoltaic EL image
(e). MSR enhancement non-defective photovoltaic EL image
(f). MSR enhancement defective (line crack) photovoltaic EL image
(g). MSR enhancement defective (star crack) photovoltaic EL image
(h). MSR enhancement defective (soiling) photovoltaic EL image
(i). MSR2 enhancement non-defective photovoltaic EL image
(j). MSR2 enhancement defective (line crack) photovoltaic EL image
(k). MSR2 enhancement defective (star crack) photovoltaic EL image
(l). MSR2 enhancement defective (soiling) photovoltaic EL image

Fig 2. Comparison of original and enhanced photovoltaic EL images using MSR and MSR2.

On the other hand, MSR2 provided even better contrast and brought out finer details, making defects more prominent and easier to detect. Figs. 2(i) to (l) illustrate the impact of MSR2, where the defects, such as line cracks, star cracks, and soiling, are displayed with greater clarity. MSR2 effectively preserved critical image features and addressed illumination challenges more efficiently than MSR, ensuring that even subtle details were captured. Although MSR2 also introduced minor distortions, they were less pronounced and had a minimal effect on the overall image quality, ensuring that defect detection was not compromised.

Overall, both MSR and MSR2 significantly enhance defect detection in photovoltaic EL images, but MSR2 stands out as the more effective technique. It provides

better contrast, preserves finer details, and handles illumination variations more effectively, all while introducing fewer distortions. This makes MSR2 a more reliable choice for improving the visibility of defects and ensuring accurate analysis of photovoltaic cells.

Table 5. Performance of original on CNN and nine pre-trained models for photovoltaic EL images.

Evalution Metric / Enhancement Method	Accuracy	Precision	Sensitivity	Specificity	F1-Score
CNN	84.73	83.60	86.40	83.05	84.98
AlexNet	90.90	89.06	93.25	88.55	91.11
DarkNet-53	92.55	90.37	95.25	89.85	92.75
DensetNet-201	93.08	91.64	94.80	91.35	93.19
EfficientNet-b0	92.45	90.05	**95.45**	89.45	92.67
GoogLeNet	92.30	90.56	94.45	90.15	92.46
ResNet-101	**93.50**	93.12	94.00	93.05	**93.56**
SqueezeNet	88.45	84.80	93.70	83.20	89.03
VGG-19	91.62	**96.48**	86.40	**96.85**	91.16
Xception	92.47	93.14	91.70	93.25	92.42

3.1.2 Comparative Analysis of Image Enchancement Techniques with CNN and Deep Pre-Trained Models

This section evaluates the influence of MSR and MSR2 image enhancement techniques on the performance of CNN and nine various deep pre-trained models for detecting defects in photovoltaic EL images. The objective is to determine the most effective combination of enhancement techniques with deep learning models for achieving superior accuracy and reliability in distinguishing defective from non-defective cells. The results are presented in Tables 5, 6, and 7, which detail performance metrics across different scenarios.

In Table 6, based on the performance metrics, DarkNet-53 emerges as the overall best-performing model across the majority of evaluation metrics, achieving the highest accuracy, sensitivity and F1-Score. AlexNet performs excellently in precision and specificity. Based on these results, DarkNet-53 is the most consistent and reliable model for photovoltaic EL image classification when using the MSR enhancement method.

Table 6. Performance of MSR on CNN and nine pre-trained models for photovoltaic EL images.

Evalution Metric / Enhancement Method	Accuracy	Precision	Sensitivity	Specificity	F1-Score
CNN	85.45	84.32	87.10	83.80	85.69
AlexNet	91.53	**95.71**	86.95	**96.10**	91.12
DarkNet-53	**93.65**	93.43	**93.90**	93.40	**93.67**
DensetNet-201	93.30	93.39	93.20	93.40	93.29
EfficientNet-b0	92.90	94.36	91.20	94.55	92.75
GoogLeNet	92.83	93.46	92.10	93.55	92.77
ResNet-101	93.60	94.54	92.55	94.65	93.53
SqueezeNet	89.15	87.39	91.50	86.80	89.40
VGG-19	93.25	94.00	92.40	94.10	93.19
Xception	92.47	93.10	91.75	93.20	92.42

In Table 7, based on the performance metrics, DarkNet-53 stands out with the highest accuracy (94.55%) and F1-score (94.43%). However, AlexNet demonstrated the highest precision (97.20%) and specificity (97.50%), while VGG-19 achieved the highest sensitivity (94.45%). Although DarkNet-53 performed consistently well across most metrics, each model had strengths in different areas, with AlexNet excelling in precision and specificity and VGG-19 in sensitivity. Overall, DarkNet-53 appears to be the most balanced and effective model for defect detection in photovoltaic EL images.

Lower-depth models, such as AlexNet, SqueezeNet, and EfficientNet-b0, generally exhibit good performance with lower computational demands, making them suitable for real-time applications. However, these models have limitations in capturing complex features in photovoltaic EL images. For example, AlexNet demonstrates a high precision and specificity with MSR2 (97.20% and 97.50%, respectively), but its overall accuracy (92.08%) and sensitivity (86.65%) are lower compared to the more complex models. SqueezeNet and EfficientNet-b0 also perform reasonably well but struggle to match the accuracy of deeper models, as seen in Table 7, where their accuracy is 89.67% and 93.22%, respectively. While these models are computationally efficient, they are outperformed by deeper models in terms of overall classification performance.

Table 7. Performance of MSR2 on CNN and nine pre-trained models for photovoltaic EL images.

Evalution Metric / Enhancement Method	Accuracy	Precision	Sensitivity	Specificity	F1-Score
CNN	86.67	84.81	89.35	84.00	87.02
AlexNet	92.08	**97.20**	86.65	**97.50**	91.62
DarkNet-53	**94.55**	96.60	92.35	96.75	**94.43**
DensetNet-201	93.40	94.20	92.50	94.30	93.34
EfficientNet-b0	93.22	94.96	91.35	95.15	93.12
GoogLeNet	93.03	93.00	93.05	93.00	93.03
ResNet-101	93.70	95.86	91.35	96.05	93.55
SqueezeNet	89.67	88.28	91.50	87.85	89.86
VGG-19	93.67	93.01	**94.45**	92.90	93.72
Xception	93.05	93.26	92.75	93.30	93.01

Medium-depth models, including GoogLeNet, DarkNet-53, and VGG-19, offer a balance between computational efficiency and performance. Among these, DarkNet-53 stands out with the highest accuracy (94.55%) and F1-score (94.43%) in Table 7, when enhanced with MSR2. It also performs exceptionally well in terms of specificity (96.75%) and precision (96.60%). This model captures complex defect patterns more effectively than the lower-depth models while maintaining computational efficiency. VGG-19, while slightly lower in overall accuracy (93.67%), excels in sensitivity (94.45%) and specificity (92.90%) with MSR2, highlighting its ability to correctly identify defective areas. GoogLeNet shows balanced performance across metrics, achieving an accuracy of 93.03%, but it does not outperform DarkNet-53 in terms of overall performance.

Higher-depth models, such as DenseNet-201, ResNet-101, and Xception, excel in learning detailed features and hierarchical representations, providing the best performance for defect detection. ResNet-101 achieves the highest accuracy (93.50%) and F1-score (93.56%) in the original dataset (Table 5), making it highly effective at detecting complex defects. DenseNet-201 and Xception also perform very well, with DenseNet-201 achieving a strong F1-score of 93.34% and Xception reaching an accuracy of 93.05%. These models are able to handle more intricate patterns in the images, providing superior defect detection compared to the lower and medium-depth models.

In conclusion, while lower-depth models like AlexNet and EfficientNet-b0 provide good results with efficient computation, they are outperformed by medium-depth and higher-depth models. Among these, DarkNet-53 is the most well-rounded performer, consistently achieving the highest overall accuracy, precision, and F1-score. ResNet-101 and DenseNet-201 also offer excellent performance but with slightly lower precision and specificity than DarkNet-53. Thus, for optimal defect detection in photovoltaic EL images, medium-depth models like DarkNet-53 provide the best results, especially when enhanced with MSR2.

3.1.3 Confusion Matrix Analysis of Image Enhancement Techniques with CNN and Deep Pre-Trained Models

This section presents a detailed analysis of the confusion matrix results for the performance of CNN and various pre-trained models using the MSR2 image enhancement technique. The confusion matrix provides essential information regarding the number of TP, TN, FP, and FN, which are crucial for evaluating the model's classification performance in detecting defects in photovoltaic EL images.

Fig. 3(a) shows the CNN performance with MSR2 enhancement. The CNN achieves an accuracy of 86.67%, with 1,787 true positives, 1,680 true negatives, 213 false positives, and 320 false negatives. Despite having moderate accuracy, CNN experiences a higher number of false positives, leading to a slightly less reliable performance compared to other models.

Fig. 3(b) presents AlexNet performance with MSR2 enhancement. AlexNet achieves an accuracy of 92.08%, with 1,733 true positives, 1,950 true negatives, 267 false positives, and 50 false negatives. This model demonstrates a significant improvement in accuracy compared to CNN, with fewer false negatives and a well-balanced performance in detecting both defective and non-defective photovoltaic cells.

Fig. 3(c) presents DarkNet-53 performance with MSR2 enhancement. DarkNet-53 achieves an accuracy of 94.55%, with 1,847 true positives, 1,935 true negatives, 153 false positives, and 65 false negatives. This model demonstrates exceptional performance, significantly improving accuracy while maintaining a low number of false positives and false negatives. DarkNet-53 stands out for its ability to accurately detect defects in photovoltaic cells with minimal misclassification, making it one of the top performers among the pre-trained models tested.

Fig. 3(d) presents DenseNet-201 performance with MSR2 enhancement. DenseNet-201 achieves an accuracy of 93.40%, with 1,850 true positives, 1,886 true negatives, 150 false positives, and 14 false negatives. The model demonstrates a strong ability to

detect defects, with a very low number of false negatives, indicating its effectiveness in identifying defective photovoltaic cells. Despite a slightly higher number of false positives, DenseNet-201 performs well, highlighting its reliability and high accuracy in the defect detection task when using the MSR2 enhancement method.

Fig. 3(e) presents EfficientNet-b0 performance with MSR2 enhancement. EfficientNet-b0 achieves an accuracy of 93.22%, with 1,827 true positives, 1,903 true negatives, 173 false positives, and 97 false negatives. The model shows strong performance, particularly in its ability to correctly classify non-defective cells, as evidenced by the high number of true negatives. While it has a moderate number of false positives, its overall accuracy and the relatively low number of false negatives indicate that EfficientNet-b0 effectively detects defects in photovoltaic cells when using the MSR2 enhancement technique.

Fig. 3(f) presents GoogLeNet performance with MSR2 enhancement. GoogLeNet achieves an accuracy of 93.03%, with 1,861 true positives, 1,860 true negatives, 140 false positives, and 139 false negatives. This model demonstrates a high level of performance in defect detection, maintaining a well-balanced number of true positives and true negatives. The relatively low number of false positives and false negatives suggests that GoogLeNet, when enhanced with MSR2, delivers reliable and accurate classification of photovoltaic defects, while maintaining a good balance between sensitivity and specificity.

Fig. 3(g) presents ResNet-101 performance with MSR2 enhancement. ResNet-101 achieves an accuracy of 93.70%, with 1,827 true positives, 1,921 true negatives, 173 false positives, and 79 false negatives. This model demonstrates strong performance, with a high number of true positives and true negatives, indicating its reliability in distinguishing between defective and non-defective photovoltaic cells. The relatively low false positive and false negative counts highlight the model's efficiency in defect detection, making it a robust choice for classification tasks with the MSR2 enhancement method.

Fig, 3(h) presents SqueezeNet performance with MSR2 enhancement. SqueezeNet achieves an accuracy of 89.67%, with 1,830 true positives, 1,757 true negatives, 170 false positives, and 243 false negatives. Although the model demonstrates a decent accuracy, the higher number of false negatives indicates that it may be less sensitive to detecting defective photovoltaic cells compared to other models. This suggests that while SqueezeNet performs reasonably well, it may require further optimization to reduce misclassification rates, particularly false negatives, for improved reliability in defect detection.

Fig. 3(i) presents VGG-19 performance with MSR2 enhancement. VGG-19 achieves an accuracy of 93.67%, with 1,895 true positives, 1,899 true negatives, 105 false positives, and 101 false negatives. This model exhibits strong performance, particularly with a high number of true positives and true negatives, reflecting its ability to accurately classify both defective and non-defective photovoltaic cells. The relatively low number of false positives and false negatives highlights VGG-19's effectiveness in defect detection, making it one of the top-performing models in terms of classification accuracy and reliability.

Fig. 3(j) presents Xception performance with MSR2 enhancement. Xception achieves an accuracy of 93.67%, with 1,855 true positives, 1,866 true negatives, 145 false positives, and 134 false negatives. The model demonstrates a balanced performance with a relatively low number of false positives and false negatives, reflecting its ability to effectively differentiate between defective and non-defective photovoltaic cells. While its accuracy is slightly lower than that of VGG-19, Xception still performs well, with high reliability in both classification categories.

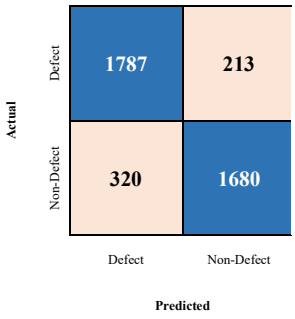

(a). CNN performance with MSR2 enhancement

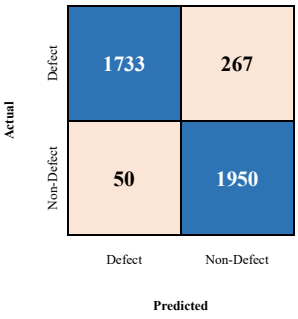

(b). AlexNet performance with MSR2 enhancement

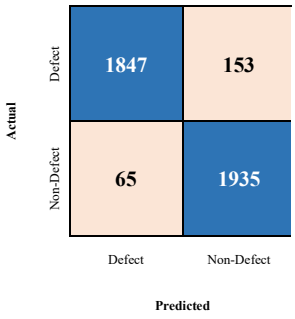

(c). DarkNet-53 performance with MSR2 enhancement

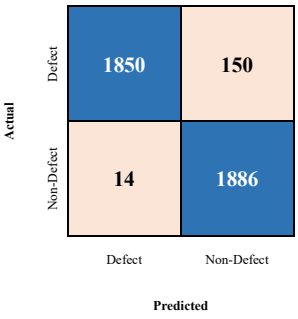

(d). DenseNet-201 performance with MSR2 enhancement

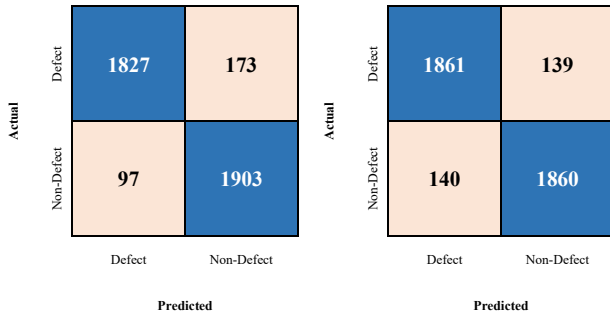

(e). EfficientNet-b0 performance with MSR2 enhancement

(f). GoogLeNet performance with MSR2 enhancement

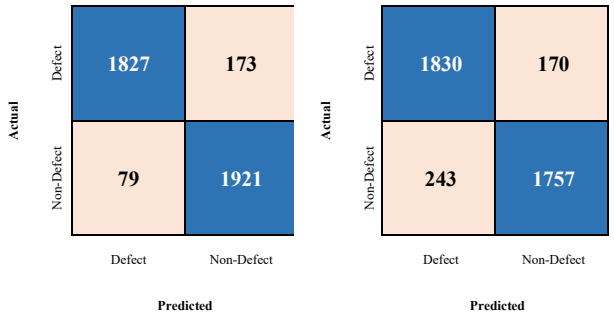

(g). ResNet-101 performance with MSR2 enhancement

(h). SqueezeNet performance with MSR2 enhancement

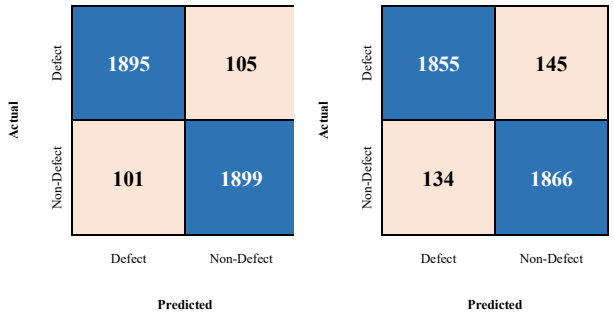

(i). VGG-19 performance with MSR2 enhancement

(j). Xception performance with MSR2 enhancement

Fig 3. Confusion matrix analysis of CNN and nine pre-trained models with MSR2 enhancement.

Based on the results, the performance of various models with and without the MSR2 enhancement technique provides valuable insights into the influence of model complexity on photovoltaic defect detection.

4 Conclusions

This study evaluated the performance of CNN and a range of pre-trained models, categorized into lower, mid, and higher-complexity architectures, for defect detection in photovoltaic EL images. The proposed image enhancement technique, MSR2, was applied to improve detection accuracy across all models. The confusion matrix analysis confirmed that MSR2 effectively reduced false positives and false negatives, with the most significant improvements observed in the mid- and higher-complexity models.

Among the models tested, DarkNet-53 emerged as the top performer, achieving the highest accuracy and overall performance across all evaluation metrics. It consistently outperformed other models, including VGG-19, which was the second-best performer. This indicates that mid-complexity models, such as DarkNet-53, benefit most from the MSR2 enhancement, providing the most accurate and reliable defect detection for photovoltaic images. VGG-19, although performing exceptionally well, was outperformed by DarkNet-53 in terms of overall accuracy and other key metrics.

In conclusion, this paper demonstrates that MSR2 is an effective image enhancement technique, significantly improving the performance of mid- and higher-complexity deep learning models. Among the models tested, DarkNet-53 emerged as the most suitable for accurate and reliable photovoltaic cell defect detection, making it the preferred model for this task.

Conflict of Interest

The authors declare no conflict of interest.

Author Contributions

Research and Investigation, H.S.M.M.; methodology, H.S.M.M., A.S.A.N., and M.H.A.N.; original draft preparation, H.S.M.M; revise and editing, A.S.A.N.; M.H.A.N., and K.A.R.; supervision, A.S.A.N., and M.F.N.T.; verification, M.F.N.T., and M.H.A.N., and All authors have read and agreed to the published version of the manuscript.

Funding

This research did not receive any specific grant from funding agencies in the public, commercial, or not-for-profit sectors.

Informed Consent Statement

Not applicable.

References

[1] B. Su, H. Chen, Y. Zhu, W. Liu, and K. Liu, "Classification of Manufacturing Defects in Multicrystalline Solar Cells with Novel Feature Descriptor," *IEEE Trans. Instrum. Meas.*, vol. 68, no. 12, pp. 4675–4688, 2019, doi: 10.1109/TIM.2019.2900961.

[2] A. Zotin and A. Zotin, "Fast Algorithm of Image Enhancement based on Multi-Scale Fast Algorithm of Image Enhancement based on Multi-Scale Retinex Retinex," *Procedia Comput. Sci.*, vol. 131, pp. 6–14, 2018, doi: 10.1016/j.procs.2018.04.179.

[3] C. Lee, J. Shih, and C. Lien, "Adaptive Multiscale Retinex for Image Contrast Enhancement," *2013*

Int. Conf. Signal-Image Technol. Internet-Based Syst., pp. 43–50, 2013, doi: 10.1109/SITIS.2013.19.

[4] S. Fan *et al.*, "A novel image enhancement algorithm to determine the dust level on photovoltaic (PV) panels," *Renew. Energy*, vol. 201, no. P1, pp. 172–180, 2022, doi: 10.1016/j.renene.2022.10.073.

[5] Z. Meng, S. Xu, L. Wang, Y. Gong, X. Zhang, and Y. Zhao, "Defect object detection algorithm for electroluminescence image defects of photovoltaic modules based on deep learning," *Energy Sci. Eng.*, vol. 10, no. 3, pp. 800–813, 2022, doi: 10.1002/ese3.1056.

[6] I. Zyout and A. Oatawneh, "Detection of PV Solar Panel Surface Defects using Transfer Learning of the Deep Convolutional Neural Networks," *2020 Adv. Sci. Eng. Technol. Int. Conf. ASET 2020*, 2020, doi: 10.1109/ASET48392.2020.9118382.

[7] H. Li, "Research on Surface Defect Detection of Solar PV Panels Based on Pre-Training Network and Feature Fusion," *IOP Conf. Ser. Earth Environ. Sci.*, 2021, doi: 10.1088/1755-1315/651/2/022071.

[8] S. Deitsch *et al.*, "Automatic Classification of Defective Photovoltaic Module Cells in Electroluminescence Images," *Sol. Energy*, vol. 185, no. July, pp. 455–468, 2019, doi: 10.1016/j.solener.2019.02.067.

[9] M. W. Akram *et al.*, "CNN based Automatic Detection of Photovoltaic Cell Defects in Electroluminescence Images," *Energy*, vol. 189, p. 116319, 2019, doi: 10.1016/j.energy.2019.116319.

[10] A. M. Karimi *et al.*, "Automated Pipeline for Photovoltaic Module Electroluminescence Image Processing and Degradation Feature Classification," *IEEE J. Photovoltaics*, vol. 9, no. 5, pp. 1324–1335, 2019, doi: 10.1109/JPHOTOV.2019.2920732.

[11] M. Mayr, M. Hoffmann, A. Maier, and V. Christlein, "Weakly Supervised Segmentation of Cracks on Solar Cells using Normalized Lp Norm," in *2019 IEEE International Conference on Image Processing (ICIP)*, 2019, pp. 1885–1889.

[12] J. Fioresi *et al.*, "Automated Defect Detection and Localization in Photovoltaic Cells using Semantic Segmentation of Electroluminescence Images," *IEEE J. Photovoltaics*, vol. 12, no. 1, pp. 53–61, 2021.

[13] C. J. Brabec *et al.*, "A Benchmark for Visual Identification of Defective Solar Cells in Electroluminescence Imagery," 2018. [Online]. Available: https://api.semanticscholar.org/CorpusID:215885514

[14] S. Deitsch *et al.*, "Segmentation of Photovoltaic Module Cells in Uncalibrated Electroluminescence Images," *Mach. Vis. Appl.*, vol. 32, no. 4, pp. 1–23, 2021, doi: 10.1007/s00138-021-01191-9.

[15] B. Su, H. Chen, Y. Zhu, W. Liu, and K. Liu, "Classification of Manufacturing Defects in Multicrystalline Solar Cells With Novel Feature Descriptor," *IEEE Trans. Instrum. Meas.*, vol. 68, no. 12, pp. 4675–4688, 2019, doi: 10.1109/TIM.2019.2900961.

[16] B. Su, Z. Zhou, and H. Chen, "PVEL-AD: A Large-Scale Open-World Dataset for Photovoltaic Cell Anomaly Detection," *IEEE Trans. Ind. Informatics*, vol. 19, no. 1, pp. 404–413, 2023, doi: 10.1109/TII.2022.3162846.

[17] B. Su, H. Chen, and Z. Zhou, "BAF-Detector: An Efficient CNN-Based Detector for Photovoltaic Cell Defect Detection," *IEEE Trans. Ind. Electron.*, vol. PP, p. 1, 2021, doi: 10.1109/TIE.2021.3070507.

[18] B. Su, H. Chen, P. Chen, G.-B. Bian, kun Liu, and W. Liu, "Deep Learning-Based Solar-Cell Manufacturing Defect Detection With Complementary Attention Network," *IEEE Trans. Ind. Informatics*, vol. PP, p. 1, 2020, doi: 10.1109/TII.2020.3008021.

[19] F. N. Shaari, "Deep CNN-LSTM Network Integration for COVID- 19 Classification," *2023 IEEE 2nd Natl. Biomed. Eng. Conf.*, pp. 142–147, 2023, doi: 10.1109/NBEC58134.2023.10352632.

[20] J. Zhou, J. Yao, W. Zhang, and D. Zhang, "Multi-Scale Retinex-Based Adaptive Gray-Scale Transformation Method for Underwater Image Enhancement," *Multimed. Tools Appl.*, vol. 81, no. 2, pp. 1811–1831, 2022, doi: 10.1007/s11042-021-11327-8.

[21] M. Ali *et al.*, "Pneumonia Detection Using Chest Radiographs with Novel EfficientNetV2L Model," *IEEE Access*, vol. 12, no. February, pp. 34691–34707, 2024, doi: 10.1109/ACCESS.2024.3372588.

[22] S. I. Safie *et al.*, "Comparison of SqueezeNet and DarkNet-53 based YOLO-V3 Performance for Beehive Intelligent Monitoring System," *2023 IEEE 13th Symp. Comput. Appl. Ind. Electron.*, pp. 62–65, 2023, doi: 10.1109/ISCAIE57739.2023.10165285.

[23] A. Sameerunnisa, "Brain Tumor Classification using EfficientNet-B0 Model," *2022 2nd Int. Conf. Adv. Comput. Innov. Technol. Eng.*, pp. 2503–2509, 2022, doi: 10.1109/ICACITE53722.2022.9823526.

[24] C. Szegedy *et al.*, "Going Deeper with Convolutions," *Proc. IEEE Comput. Soc. Conf. Comput. Vis. Pattern Recognit.*, vol. 07-12-June, pp. 1–9, 2015, doi: 10.1109/CVPR.2015.7298594.

[25] H. Wang, F. Zhang, and L. Wang, "Fruit Classification Model Based on Improved Darknet53 Convolutional Neural Network," pp. 881–884, 2020, doi: 10.1109/ICITBS49701.2020.00194.

[26] F. N. Shaari, A. Salihah, A. Nasir, and W. A. Mustafa, "Variant Histogram Equalization based Enhancement to Transfer Learning in Detection of COVID-19 Chest X-Ray Images," *2023 IEEE 2nd Natl. Biomed. Eng. Conf.*, pp. 158–163, 2023, doi: 10.1109/NBEC58134.2023.10352580.

[27] T. B. Beijing, T. B. Beijing, T. B. Beijing, and J. Mao, "Research on ResNet101 Network Chemical Reagent Label Image Classification Based on Transfer Learning," pp. 354–358, 2020.

[28] F. Chollet, "Xception: Deep Learning with Depthwise Separable Convolutions," *Proc. - 30th IEEE Conf. Comput. Vis. Pattern Recognition, CVPR 2017*, vol. 2017-Janua, pp. 1800–1807, 2017, doi: 10.1109/CVPR.2017.195.

Biographies

Hanim Suraya Mohd Mokhtar received a B. Electrical Eng. Technology (Hons) (Robotic and Automation Technology) degree in Mechatronics Engineering at Universiti Malaysia Perlis in 2023. She is currently pursuing his Ph. D in Mechatronics Engineering at Universiti Malaysia Perlis. Her research interests include image processing and deep learning.

Aimi Salihah Abdul Nasir received her B.Eng (Hons) degree in Mechatronic Engineering from Universiti Malaysia Perlis (UniMAP) in 2009. In 2015, she obtained her Ph.D. in Biomedical Electronic Engineering from the same university, specialized in medical image processing with a focus on the clustering analysis. Her research interests include image processing, medical image analysis, artificial intelligence, and deep learning.

Mohammad Faridun Naim Tajuddin received the B.Eng. and M.Eng. degrees from the University of Malaya (UM), Malaysia, in 2004 and 2007, respectively, and the Ph.D. degree from Universiti Teknologi Malaysia (UTM), Johor, Malaysia, in 2015. He is currently an Associate Professor with the Faculty of Elctrical Engineering Technology, Universiti Malaysia Perlis (UniMAP). He has published refereed manuscripts in various reputable international journals. His research interests include power electronics control,photovoltaic modeling and control, intelligent control, and optimization techniques. He acts as a Reviewer for various reputed journals, such as IEEE and Elsevier *Applied Energy, Renewable* and *Sustainable Energy Review*s, *Neurocomputing*, and *Energy Reports*.

Muhammad Hafeez Abdul Nasir received his Bachelor of Design Studies and Master of Architecture from the University of Adelaide, South Australia. In 2021, he obtained his Ph.D specializing in interdisciplinary architectural research from Universiti Sains Malaysia (USM). His expertise in research is interdisciplinary.

Kumuthawathe Anando-Rao received her B.Eng (Hons) degree in Electrical Engineering from Universiti Malaysia Perlis (UniMAP) and Ph.D in Electrical Engineering from the same university. Her research interests include renewable energy and energy management.